Integrative Biology

PAPER

Cite this: *Integr. Biol.*, 2017, 9, 751

Pheomelanin molecular vibration is associated with mitochondrial ROS production in melanocytes and systemic oxidative stress and damage†

Ismael Galván, *[a] Alberto Jorge[b] and María García-Gil[c]

Received 14th June 2017,
Accepted 9th July 2017

DOI: 10.1039/c7ib00107j

rsc.li/integrative-biology

Vibrations in covalent bonds affect electron delocalization within molecules, as reported in polymers. If synthesized by living cells, the electron delocalization of polymers affects the stabilization of cellular free radicals, but biomolecular vibration has never been considered a potential source of cytotoxicity. Here we show that the vibrational characteristics of natural pheomelanin and eumelanin contribute to feather color expression in four poultry breeds with different melanin-based pigmentation patterns, but only the vibrational characteristics of pheomelanin are related to the production of reactive oxygen species (ROS) in the mitochondria of melanocytes and to systemic levels of cellular oxidative stress and damage. This association may be explained by the close physical contact existing between mitochondria and melanosomes, and reveals an unprecedented factor affecting the viability of organisms through their pigmentation. These findings open a new avenue for understanding the mechanism linking pheomelanin synthesis to human melanoma risk.

Insight, innovation, integration

We reveal that vibration in the bonds of pheomelanin affects the prevalence of free radicals in the mitochondria of melanocytes. Mitochondrial free radicals, in turn, favor cellular oxidative stress and damage in the entire organism. These findings may be explained by the influence of the vibrational characteristics of molecules on their electron delocalization, and by the physical contact between mitochondria and the organelles where melanin synthesis takes place. Our study shows that molecular vibration is an unsuspected source of cellular and organismal damage, and should be considered as a potential factor by which pheomelanin synthesis may promote melanoma and other disorders.

Introduction

Molecules exhibit constant movement due to vibrations in their covalent bond network. When molecules interact with light, these vibrations make that part of the infrared (IR) radiation is absorbed, and thus IR asborbance spectra provide information on how molecules vibrate.[1] Similar and complementary information is obtained from the portion of IR radiation that is inelastically scattered during the interaction of molecules with light, which is termed Raman scattering. Therefore, Raman spectroscopy represents a useful characterizing tool that helps to determine how molecules vibrate and to identify molecules[1] (Fig. 1).

However, it has never been considered that, if molecules are synthesized by living cells (*i.e.* biomolecules), their vibrational characteristics could have physiological consequences that may compromise cell viability. This is because vibrational motions may influence the electronic structure of molecules, thus affecting their electronic properties. Indeed, the broadening of electronic spectra stems from the nuclear dynamics of the solute and the environment.[2] Molecular vibration may thus affect electronic properties of molecules such as the density of electrons around their constitutive atoms (*i.e.*, electron delocalization).[3] Outstanding evidence for the interaction between molecular vibration and electron delocalization is provided by works on benzene, as the variation in the vibrational characteristics of this molecule, even that occurring at room temperature, is associated with fluctuations in π-electron delocalization and thus determines its aromaticity.[4] These effects

[a] *Department of Evolutionary Ecology, Doñana Biological Station – CSIC, 41092 Sevilla, Spain. E-mail: galvan@ebd.csic.es*
[b] *Laboratory of Non-Destructive Analytical Techniques, National Museum of Natural Sciences – CSIC, 28006 Madrid, Spain*
[c] *Department of Animal Genetic Improvement, Institute for Agricultural and Food Research and Technology (INIA), 28040 Madrid, Spain*

† Electronic supplementary information (ESI) available. See DOI: 10.1039/c7ib00107j

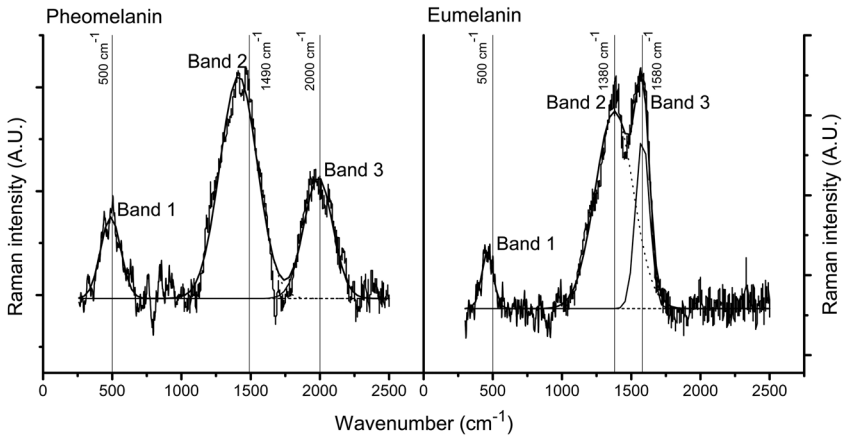

Fig. 1 Raman spectra of melanin pigments. The shape of the spectra (*i.e.* position of the main bands in the wavenumber range shown) allows one to assign the signal to one of the two main chemical forms of melanin, *i.e.* pheomelanin or eumelanin. The band at about 500 cm^{-1} (band 1) in both pheomelanin and eumelanin is assigned to the out-of-plane deformation of hexagonal carbon rings in the molecule structure. Band 2, located at about 1490 cm^{-1} in pheomelanin and at about 1380 cm^{-1} in eumelanin (band 2), is assigned to the stretching vibration of hexagonal rings. The assignment of pheomelanin's band 3 at the region of 2000 cm^{-1} is still not fully understood, while eumelanin's band 3 at about 1580 cm^{-1} is assigned to the stretching of three of the six C–C bonds within the rings. See ref. 20 and 22 for details. Figure adapted from ref. 20.

of vibrational characteristics on electron delocalization have also been demonstrated in polymers,[5] which are particularly relevant for the study of possible physiological effects of molecular vibration because it is also known that electron delocalization of some biopolymers affects the stabilization (*i.e.* cytotoxicity) of free radicals with which they interact.[6,7] This raises the question, never considered in biology, of whether the vibrational characteristics of biopolymers or any other biomolecules influence the prevalence of cytotoxic free radicals when interacting with them.

We explored this possibility in melanins, natural biopolymers that are synthesized by cells termed melanocytes in vertebrates and constitute the main molecules responsible for animal pigmentation. The recent discovery of fibrillar bridges that connect mitochondria with the organelles where melanin synthesis takes place in melanocytes (*i.e.* melanosomes), and on which the melanogenesis process depends,[8] makes melanin molecular vibration a good model to investigate potential effects on mitochondrial reactive oxygen species (ROS). Mitochondria are the organelles where cellular respiration takes place, a process that produces, particularly during the electron transport chain, the most significant amounts of ROS in eukaryotic cells and consequently constitutes an important source of cytotoxicity.[9] Mitochondrial ROS are therefore highly relevant to the viability of organisms.

Furthermore, the sulphurated form of melanin, termed pheomelanin, has a high susceptibility to cause physiological damage, which is exerted by different mechanisms. First, early studies in the 1970s already showed that pheomelanin produces superoxide anion (*i.e.* an important ROS) when the polymer interacts with UV radiation,[10] a process leading to phototoxicity that has been characterized in detail by later studies.[11,12] Another damaging effect of pheomelanin is exerted, however, during its synthesis in melanocytes, because the sulfhydryl group of cysteine [*i.e.* one of the three constituent amino acids of the main intracellular antioxidant: glutathione (GSH)] is transferred to the pigment structure and thus the process constitutes the consumption of an important antioxidant resource. Consequently, pheomelanin production for pigmentation limits physiological performance as shown by studies on wild birds exposed to stressful environmental conditions,[13] and in humans it is involved in melanoma formation[14–18] and predicts survival in patients of malignant glioma.[19] Thus, any association between pheomelanin vibrational characteristics and mitochondrial ROS-mediated cytotoxicity may help to understand the participation of pheomelanin in these disorders.

Using melanocytes from regenerating feathers of fowl with different pigmentation phenotypes, we investigated the association between mitochondrial ROS levels and the vibrational characteristics of melanins synthesized. As melanin molecular vibration may have physiological effects beyond cellular levels and be of general relevance for the viability of organisms, we also investigated potential effects on systemic levels of oxidative stress (*i.e.* the imbalance between ROS abundance and the availability of antioxidant compounds that combat them, tipped toward the former) and damage.

Several measurements (spectral position, intensity, width at half maximum and area of the different bands) can be obtained to characterize the variability in the shape of the Raman spectra of melanins. These measurements are highly intercorrelated,[20] which prevents their analysis as predictor variables in conventional regression because of multicollinearity problems. Selecting only some of these measurements or creating synthetic variables that summarize them would lead to a loss of information, but we were able to determine the relative importance of all these measurements in explaining variation in the response variables (phenotype expression and mitochondrial ROS) by using partial least squares regression (PLSR) models.[21] PLSR is an extension of multiple regression analysis in which associations are established with components extracted from predictor variables that maximize the explained variance in the response variable. These components are defined as a linear combination of predictor

variables, so the original multidimensionality is reduced to a small number of orthogonal components to detect structure in the relationships between predictor variables and between these factors and the response variable.[21] Results obtained with PLSR are similar to those from conventional multiple regression techniques, but this method is extremely resilient to the degree of correlation between predictor variables. This makes PLSR especially useful in cases of severe multicollinearity, which is the case of Raman spectral data.[20]

Results and discussion

We quantified the vibrational characteristics of melanins in the barbs and barbules of growing feathers of 80 fowl belonging to the breeds Black Castellana, Blue Andaluza, Buff Prat and Red Villafranquina using micro-Raman spectroscopy on the basis of bands recently reported as specific Raman signals from pheomelanin and eumelanin[18,20,22] (Fig. 2). The pigmentation phenotypes of these poultry breeds virtually cover the entire phenotypic diversity that is produced by melanins[23] (Fig. 2). Only Raman signals from pheomelanin were detected in the feathers of the Buff Prat breed, only Raman signals from eumelanin were detected in the feathers of Black Castellana and Blue Andaluza breeds, and Raman signals from both pheomelanin and eumelanin were detected in the feathers of the Red Villafranquina breed. We also quantified the expression of color produced by melanins in the same feathers by reflectance spectrophotometry, and found that the vibrational characteristics (spectral position, intensity, width at half maximum and area of the different Raman bands) of both pheomelanin and eumelanin explained between 50.8 and 53.9% of variance (R^2) in color intensity between birds (Fig. 2 and Table S1, ESI†). The vibrational characteristics of melanins are therefore significant predictors of the variation in the expression of the pigmentation phenotype of fowl. Although molecules vibrate at frequencies in the IR spectral region while the visible absorption spectra of molecules (*i.e.* color) derive from the energy states of their constitutive electrons, vibrational and electronic properties of molecules interact as mentioned above. In fact, it has been theoretically demonstrated that molecular vibration can predict the visible absorption spectra of biological pigments such as flavins[24] and carotenoids[25] and even the perceived colors produced by anthraquinones.[26] This may explain the association between melanin vibrational characteristics and the expression of the pigmentation phenotype.

We isolated melanocytes from the melanin unit of the regenerating follicles of the same feathers in which the

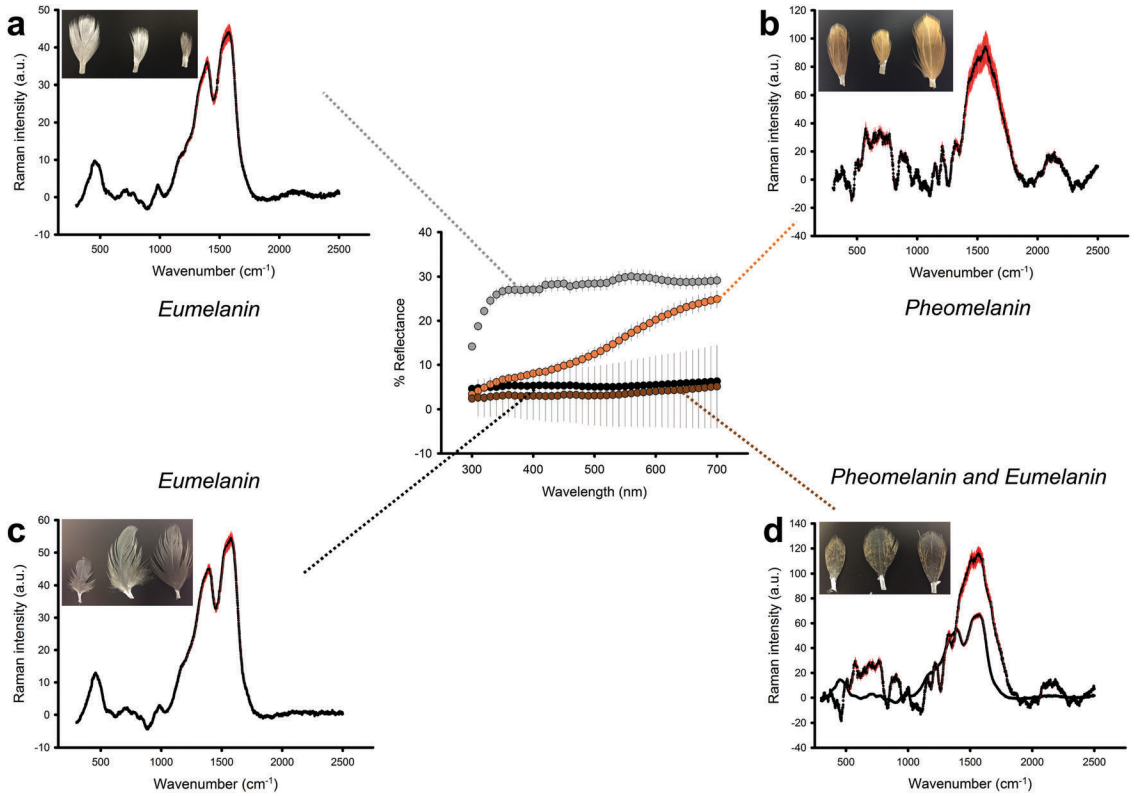

Fig. 2 Raman and reflectance spectra of feathers. The central graph shows the mean (±s.e.) reflectance of four poultry breeds. Peripheral graphs show mean (±s.e. depicted in red) intensity values of the Raman signal from pheomelanin and eumelanin in the feathers of Blue Andaluza (a), Buff Prat (b), Black Castellana (c) and Red Villafranquina (d) breeds. The inset photographs show examples of analyzed feathers. In Red Villafranquina feathers (d), the detected Raman signal from eumelanin was restricted to the black color patch, while the detected Raman signal from pheomelanin was restricted to the light brown color patch.

vibrational characteristics of melanins were analyzed, thus obtaining a direct association between melanin-synthesizing melanocytes from follicles and melanin polymers produced by them and deposited in the barbs and barbules of feathers. Live melanocytes were treated with dihydrorhodamine-123 (DHR) or MitoSOX Red (Mitosox), two dyes that produce green and yellow fluorescence, respectively, after oxidation by reactive species in the mitochondria. Mitosox is specifically oxidized by superoxide (O_2^{-})[27] and DHR is mostly oxidized by peroxynitrite (ONO_2^{-}),[28] with the latter resulting from the reaction of superoxide with nitric oxide. Thus, the fluorescence intensity of DHR and Mitosox is indicative of the amounts of superoxide, a free radical that represents one of the major ROS produced by aerobic metabolism,[9] being generated in the mitochondria of the isolated melanocytes. Although the fluorescence of Mitosox and DHR is not exclusively mediated by ROS, it is often related to relevant biological effects expected to be caused by ROS in a diversity of cells[29,30] including melanocytes,[31] which supports the use of Mitosox and DHR fluorescence as an indicator of mitochondrial ROS production. If electron delocalization in melanin polymers is related to their vibrational characteristics and affects the stabilization (*i.e.* reactivity) of free radicals in the melanocytes where melanins are produced as we hypothesize, melanin vibrational characteristics should successfully predict ROS detection in melanocytes.

The quantification of mitochondrial fluorescence by flow cytometry and subsequent statistical analyses revealed that six vibrational characteristics of pheomelanin significantly explained 21.4% of variance in DHR fluorescence after controlling for the effects of breed, sex and physical condition of fowl, and one vibrational characteristic explained 10.3% of variance in Mitosox fluorescence (Fig. 3 and Table 1). In contrast, none of the vibrational characteristics of eumelanin explained variation in either DHR or Mitosox fluorescence, which was only related to the sex of birds (Table 1). Specifically, the vibrational characteristics of pheomelanin that predict ROS levels are the spectral position and width at half maximum of the Raman band at about 500 cm^{-1} (band 1), the area of the band at about 1490 cm^{-1} (band 2), and the intensity, width at half maximum and area of the band at about 2000 cm^{-1} (band 3) (Fig. 1 and 3 and Table 1). Bands 1 and 2 are caused, respectively, by the out-of-plane deformation and the stretching vibration of the phenyl rings in the pheomelanin polymer.[22] Band 3, despite being located within the so-called 'silent region' of the Raman spectrum of biological samples, has recently been attributed to vibrational Raman signals from pheomelanin.[18] Thus, considering the sign of these predictor effects (Table 1), mitochondrial ROS production increased with the frequency of the out-of-plane deformation of phenyl rings and with the decrease in the width of this vibrational effect, with the decrease in the area of the stretching effect of phenyl rings, and with the decrease in the intensity, width and area of the still unknown vibrational effect leading to Raman band 3.

This stresses the cytotoxicity of pheomelanin, as opposed to the non-sulphurated form eumelanin, in line with previous work conducted in other species of birds and also in mammals including humans.[13,14,18] Our work, however, unveils an unsuspected molecular feature potentially contributing to the damaging nature of pheomelanin. These results suggest that ROS production in the mitochondria of melanocytes is related to the energy and mode of vibration of pheomelanin, likely because of the physical contact mediated by fibrillar bridges between melanosomes and mitochondria, on which melanogenic activity also depends.[8] This inter-organelle connection makes plausible an effect of electron delocalization of the pheomelanin polymers on the stabilization of mitochondrial ROS. In fact, a low π-electron delocalization within polymer scaffolds has been demonstrated to confer superior free radical scavenging properties (*i.e.*, higher antioxidant capacity) to synthetic melanin.[32] At this stage we cannot prove a direct

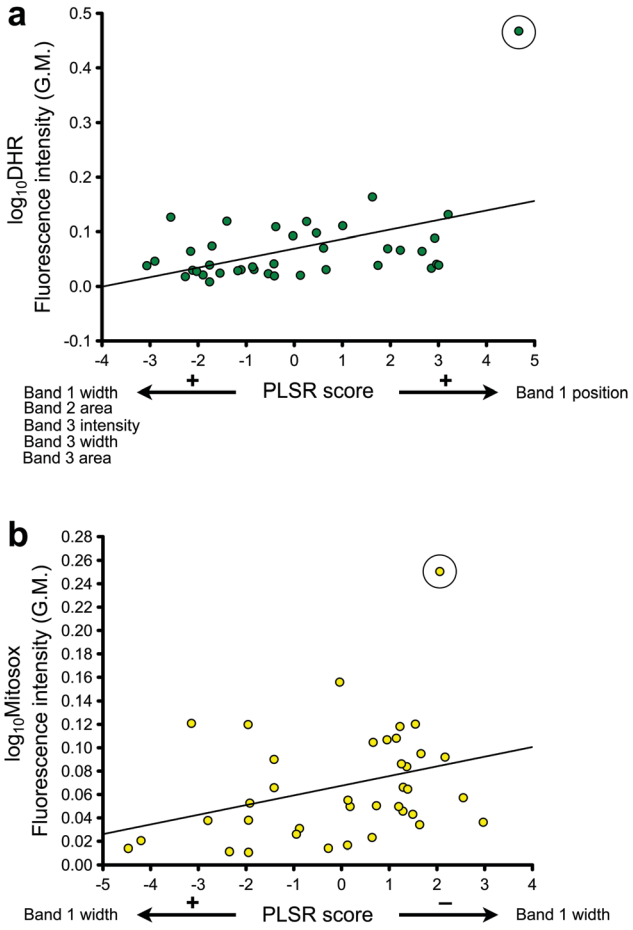

Fig. 3 Relationship between pheomelanin molecular vibration and mitochondrial ROS. PLSR scores represent the position of sampling units (*i.e.* melanocytes from individual growing feathers) along an axis composed of the predictor vibrational characteristics of pheomelanin in the same feathers. The names of predictors indicate which side of the axes increased with increasing values. Scores in (a) and (b) were obtained from two separate PLSR models for each response variable (DHR and Mitosox) and whose results are provided in Table S2 (ESI†). Correlations are statistically significant for both melanocytes treated with DHR (a; r = 0.46, P = 0.003) and with Mitosox (b; r = 0.32, P = 0.049), and remain marginally non-significant when two potential outliers with high fluorescence values (highlighted with a black circle) were removed (a: r = 0.29, P = 0.081; b: r = 0.27, P = 0.106). These potential outliers in (a) and (b) correspond to different samples. The lines are the best-fit lines.

Table 1 Relationship between melanin molecular vibration and mitochondrial ROS in melanocytes. The results of four PLSR models for DHR and Mitosox fluorescence intensity considering vibrational characteristics of pheomelanin or eumelanin are shown. Vibrational characteristics refer to the spectral position (*X*), intensity (*Y*), width at half maximum (*W*) and area (*A*) of diagnostic Raman bands 1, 2 and 3 for pheomelanin and eumelanin. Predictors whose regression coefficients are significant are marked in bold (*: $P < 0.05$, **: $P < 0.01$)

	DHR fluorescence – pheomelanin		Mitosox fluorescence – pheomelanin		DHR fluorescence – eumelanin		Mitosox fluorescence – eumelanin	
Predictor	Predictor weight	Regression coefficient	Predictor weight	Regression coefficient	Predictor weight	Regression coefficient	Predictor weight	Regression coefficient
*X*1	**−0.20***	$\mathbf{2.53 \times 10^{-4}}$	−0.39	-3.40×10^{-4}	0.05	4.80×10^{-4}	−0.20	4.80×10^{-4}
*Y*1	0.09	-1.31×10^{-4}	−0.45	-1.16×10^{-4}	0.02	1.80×10^{-4}	0.09	1.80×10^{-4}
*W*1	**−0.08***	$\mathbf{-4.13 \times 10^{-4}}$	**−0.35***	$\mathbf{-2.77 \times 10^{-4}}$	0.10	3.50×10^{-4}	−0.08	3.50×10^{-4}
*A*1	0.00	-1.00×10^{-6}	−0.29	-1.00×10^{-6}	−0.03	-3.00×10^{-6}	0.00	-3.00×10^{-6}
*X*2	−0.15	2.34×10^{-4}	0.01	6.00×10^{-6}	−0.15	-1.25×10^{-3}	−0.15	-1.25×10^{-3}
*Y*2	0.03	-6.20×10^{-5}	−0.30	-2.90×10^{-5}	−0.07	-1.94×10^{-4}	0.03	-1.94×10^{-4}
*W*2	0.25	-3.93×10^{-4}	−0.13	-5.70×10^{-5}	−0.17	-5.63×10^{-4}	0.25	-5.63×10^{-4}
*A*2	**0.09***	$\mathbf{-1.00 \times 10^{-6}}$	−0.32	0.00	−0.11	-2.00×10^{-6}	0.09	-2.00×10^{-6}
*X*3	−0.18	1.49×10^{-4}	0.15	3.70×10^{-5}	0.17	1.96×10^{-3}	−0.18	1.96×10^{-3}
*Y*3	**0.00***	$\mathbf{-3.02 \times 10^{-4}}$	0.02	1.10×10^{-5}	−0.11	-2.48×10^{-4}	0.00	-2.48×10^{-4}
*W*3	**0.01****	$\mathbf{-4.50 \times 10^{-4}}$	−0.13	-1.47×10^{-4}	−0.17	-6.14×10^{-4}	0.01	-6.14×10^{-4}
*A*3	**0.02***	$\mathbf{-4.00 \times 10^{-6}}$	0.14	1.00×10^{-6}	−0.09	-1.00×10^{-6}	0.02	-1.00×10^{-6}
Breed	—	-7.41×10^{-3}	—	2.40×10^{-3}	—	-7.72×10^{-3}	—	-7.72×10^{-3}
Sex	—	-1.34×10^{-2}	—	-1.12×10^{-3}	**—***	$\mathbf{-2.47 \times 10^{-2}}$	**—****	$\mathbf{-2.47 \times 10^{-2}}$
Condition	0.09	-7.64×10^{-3}	−0.36	-9.97×10^{-4}	−0.16	-9.32×10^{-2}	0.09	-9.32×10^{-2}

causality between pheomelanin molecular vibration and reactivity of mitochondrial ROS, but the associations found here should motivate future experiments testing for this mechanism.

If not counterbalanced by antioxidants, mitochondrial ROS leads to oxidative stress and damage to cells, representing one of the main sources of cytotoxicity.[9] We therefore determined the physiological consequences of ROS production in melanocytes in terms of cellular oxidative stress and damage at a systemic level, to investigate possible general effects that may be relevant for the viability of birds and specifically for pheomelanin-related disorders such as melanoma. As an index of systemic oxidative stress, we quantified the glutathione (GSH) to oxidized glutathione (GSSG) ratio in erythrocytes, which has been reported to be low in circulating melanoma cells.[33] As an index of systemic oxidative damage, we quantified circulating levels of malondialdehyde (MDA), a product of ROS-mediated lipid peroxidation that also induces DNA damage[34] and has been reported to contribute to melanoma progression.[35] We accounted for the antioxidant capacity of birds by quantifying the activity of superoxide dismutase (SOD), the enzyme that catalyses the dismutation of superoxide into the less oxidizing species molecular oxygen (O_2) and hydrogen peroxide (H_2O_2). As hydrogen peroxide is still an important ROS causing cellular oxidative stress,[36] we further accounted for the activity of catalase, the enzyme catalysing the decomposition of hydrogen peroxide to water and molecular oxygen, and, in the analyses of MDA, for GSH levels. After controlling for the effects of these factors and for the effects of breed, sex and physical condition, we found that the GSH:GSSG ratio significantly decreased with the fluorescence intensity of both DHR and Mitosox (Fig. 4) and, accordingly, MDA levels increased with the fluorescence intensity of DHR and Mitosox (Fig. 5 and Table S2, ESI†). The amount of variance explained by the statistical models was as high as 74.9% for GSH : GSSG ratio and 83.9% for MDA levels. Thus, mitochondrial ROS levels predicted by pheomelanin vibrational characteristics produced oxidative stress and damage at a systemic level in birds.

Given the determinant role of ROS in cell senescence and death through the promotion of oxidative stress and damage,[9] our findings indicate that the vibrational characteristics of pheomelanin synthesized in melanocytes may have profound consequences for the fitness of birds. The similarity of melanogenesis in birds and mammals[37] suggests that these results are directly relevant to human melanomagenesis. Pheomelanin synthesis is probably related to melanoma risk because the sulfhydryl group of cysteine is transferred to the pigment structure and thus cysteine used for pheomelanogenesis is no longer available to play its antioxidant role as part of GSH, promoting chronic oxidative stress because of constant cysteine/GSH consumption.[15,16] This is further reinforced by the induction of GSH autooxidation by pheomelanin once the polymer is formed, which decreases GSH levels.[16,17] We suggest that the vibrational characteristics of pheomelanin should be added to these effects as another potential factor contributing to melanomagenesis. The energy and mode of vibration have been considered a characterizing feature of molecules, but the possibility of exerting physiological effects when the molecules are synthesized in cells had not been contemplated. Our study shows that the vibrational characteristics of biomolecules can have consequences for entire organisms. It must be noted that Electron Paramagnetic Resonance (EPR) spectra can obtain information on variation in electron delocalization of melanin aggregates in human skin,[38] suggesting that EPR could be used in combination with Raman spectroscopy to determine both vibrational and electronic properties of pheomelanin and thus the potential cytotoxicity of the pigment. Future studies should explore this applicability.

The strong association between the pigmentation phenotype and the molecular vibration of melanins found here makes likely the existence of a genetic regulation of the vibrational characteristics of melanin polymers synthesized in melanocytes instead of a random determination of these characteristics during melanogenesis. A genetic basis of biomolecular vibration

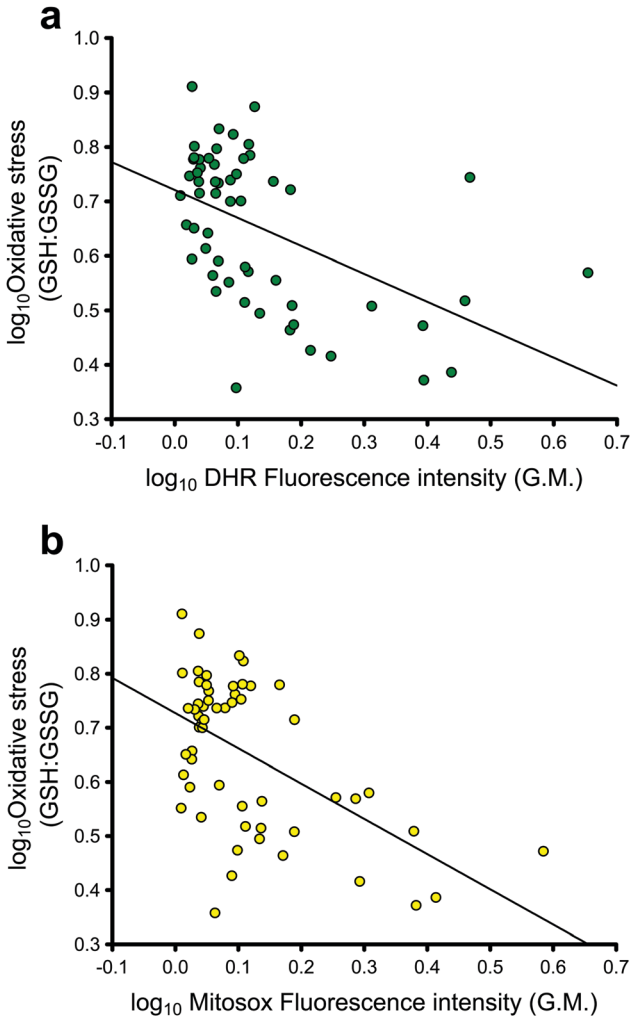

Fig. 4 Relationship between mitochondrial ROS and systemic oxidative stress. The GSH : GSSG ratio in erythrocytes was significantly and negatively correlated with the amount of ROS in melanocytes as measured by DHR fluorescence (a; $r = -0.50$, $P < 0.001$) and Mitosox fluorescence (b; $r = -0.55$, $P < 0.0001$). The lines are the best-fit lines.

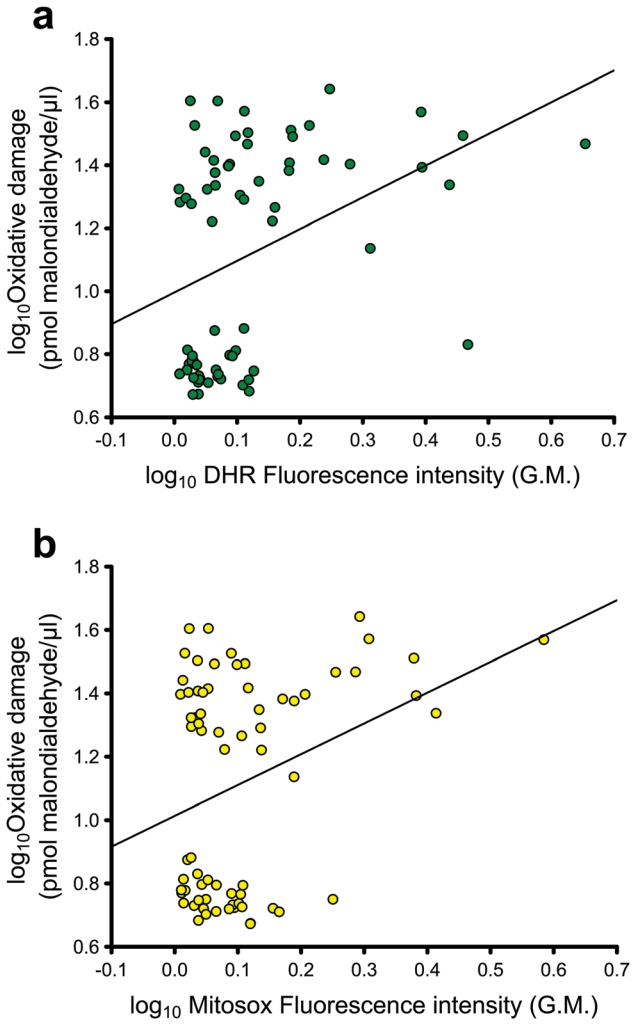

Fig. 5 Relationship between mitochondrial ROS and systemic oxidative damage. MDA values in plasma were significantly and positively correlated with the amount of ROS in melanocytes as measured by DHR fluorescence (a; $r = 0.38$, $P = 0.001$) and Mitosox fluorescence (b; $r = 0.32$, $P = 0.007$). The lines are the best-fit lines.

has never been considered, but the discovery of such hypothetical mechanism may help to modify the vibrational characteristics of natural pheomelanin. The biological receptors of molecular vibration that have been reported in *Drosophila*[39] indeed suggest that cells are provided with mechanisms that are sensitive to vibrational characteristics, thus making plausible a cellular ability to regulate the vibration of biomolecules during their synthesis. In the case of melanins, this regulation may be related to the cellular control of the assembly of polymer scaffolds, as melanin polymers with different scaffold assemblies may present different vibrational characteristics. Despite recent advances in materials science on the capacity to modify vibrational characteristics to control the chemical reactivity of molecules,[40–42] including polymers,[43] their applicability to living systems seems unaffordable. Instead, understanding the genetic mechanisms by which melanocytes synthesize pheomelanin with given scaffold assemblies and vibrational characteristics would open the possibility to create melanocytes that produce less cytotoxic pheomelanin polymers. The mechanisms by which pheomelanin scaffolds (*i.e.* benzothiazole and benzothiazine moieties) are assembled in melanosomes are still not understood,[44] but our findings should represent a new motivation to prioritize research in that direction.

Experimental

Animals

80 domestic fowl of five months of age and belonging to four native Spanish breeds (Black Castellana, Blue Andaluza, Buff Prat and Red Villafranquina) were used in the study. Variation in the pigmentation phenotype of these breeds (Fig. 2) is explained by polymorphism in the melanocortin-1 receptor (MC1R) gene.[45] The birds were maintained in 3 × 2 m indoor aviaries with *ad libitum* food and water supply under a natural light regime following conventional procedures for domestic fowl in El Encín facilities, Institute for Agricultural and Food

Research and Technology (INIA) (Madrid, Spain). These birds were raised as part of a genetic resources conservation programme started in 1975.[45] Males and females from each breed were maintained in separate aviaries. All birds were individualized with a numbered plastic ring. All experiments were performed in compliance with the relevant laws and institutional guidelines. Animals used in the study were handled according to procedures approved by the INIA Ethics Committee (ORCEEA 2015-016) and all animal experiments were performed in accordance with the Spanish Policy for Animal Protection (PROEX216/2015), which conforms to European Union Directive 86/609 regarding the protection of animals used in scientific experiments.

Experimental procedures

Birds from each breed comprised 10 males and 10 females, except the Red Villafranquina for which 20 females were used. The reason for excluding Red Villafranquina males is that this breed shows sexual plumage dichromatism and males display black coloration very similar to that of Black Castellana fowl, while females display dark brown coloration (Fig. 2). Thus, to cover the entire diversity of color phenotypes produced by melanins[23] and restrict each phenotype to a particular breed, we only included Red Villafranquina hens.

The transfer of melanocytes from the dermal papilla to the epithelial cylinder of feather follicles, from which these cells can be extracted with the feathers, occurs during feather growth.[46] Therefore, we plucked feathers from the birds to induce the growth of new feathers from which to extract melanocytes. We plucked all body feathers from an area of 30 cm^2 in the right flank of each bird. Three weeks later, when feathers were still growing but a significant part of the feather was already developed (Fig. 2), two growing feathers were plucked from each bird and immersed in phosphate-buffered saline (PBS) in separate tubes. Melanocytes from one of these feathers were treated with DHR to detect mitochondrial ROS, while melanocytes from the other feather were treated with Mitosox (see below). The analyses of mitochondrial ROS in melanocytes were conducted within 5 h after plucking the feathers.

Within 24 h after plucking the feathers, we took 1 ml of blood from the brachial vein of birds. The blood was centrifuged at 3500*g* for 5 min, and the cellular and plasma fractions were separated and stored at −80 °C until the analyses of oxidative stress and damage (see below). We also measured the body mass of birds to the nearest 50 g with a Pesola AG (Schindellegi, Switzerland) balance, and the tarsus length with a digital calliper as a measure of body size. The physical body condition of birds was calculated as the residuals of $\log_{10}$ body mass regressed against $\log_{10}$ tarsus length.

Isolation of melanocytes

To extract and isolate melanocytes from regenerating feather follicles, we followed a procedure for the extraction of melanocytes from human hair follicles,[47] with some modifications. We cut the bottommost portion of the feather follicles corresponding to the melanin unit, which represents an important reservoir of melanocytes and can be identified by a dark contrasting color.[46,47] To separate cells from the keratin matrix, the follicles were immersed in 1 ml of trypsin–EDTA solution (Sigma-Aldrich, St. Louis, MO, USA) and incubated at 37 °C for 90 min. To avoid the digestion of cells by trypsin once separated from the matrix, the feather follicles were placed in a new tube with trypsin–EDTA after every 30 min, terminating the reaction in the previous tube by adding trypsin inhibitor (Sigma-Aldrich)[43] after a short vortex to favor cell separation. The contents of all three tubes were combined and transferred to a single tube after filtration with a 70 μm cell strainer (Biologix, St. Louis, MO, USA). These tubes were centrifuged at 220*g* for 5 min, the supernatant removed and the cell pellet resuspended in 100 μl of PBS with either dihydrorhodamine-123 (DHR; Molecular Probes, Thermo Fisher Scientific, Madison, WI, USA) or MitoSOX Red (Mitosox; Molecular Probes). These cell suspensions were then incubated at 37 °C for 30 min, centrifuged at 500*g* for 5 min after adding 1.5 ml of PBS, and the supernatant was removed. Dye-treated cells were then analyzed by flow cytometry.

Mitochondrial ROS

We measured the intensity of DHR and Mitosox fluorescence from the mitochondria of melanocytes using a Guava EasyCyte Mini flow cytometer (Merck Millipore, Billerica, MA, USA). The green and yellow channels of this system detect fluorescence emission at 530 and 583 nm,[48,49] respectively, virtually coinciding with the maximum emission wavelength of DHR (529 nm) and Mitosox (580 nm). Using the Guava Express Pro software (Millipore), we calculated the total number of cells and the geometric mean (G.M.) of fluorescence after excluding debris. To obtain a measure of mean fluorescence intensity from individual melanocytes, we divided the G.M. of fluorescence intensity from the entire melanocyte population by the total number of cells.

Vibrational characteristics

Melanin polymers synthesized by melanocytes in the regenerating feather follicles are transferred to the keratin matrix of the feather branch as the feather grows.[46] We therefore investigated the vibrational characteristics of melanins deposited in the barbs and barbules of the same feathers from which melanocytes were extracted. The feathers were analyzed using a Thermo Fisher DXR confocal dispersive Raman microscope (Thermo Fisher Scientific) with a point-and-shoot Raman capability of 1 μm spatial resolution and using a near-infrared excitation laser of 780 nm.[50] Laser power was set at 5–7 mW when obtaining pheomelanin spectra, and at 1 mW when obtaining eumelanin spectra due to its higher capacity to absorb visible-infrared radiation and the consequent high tendency of eumelanin-containing tissues to get burnt.[50] In all cases, the integration time was 3 s and the number of accumulations was 8. The single spectra were obtained using a 50× confocal objective and a slit aperture of 25 μm. These conditions produced an average spectral resolution of 2.2–4.4 cm^{-1} in the wavenumber range of 150–2500 cm^{-1}. The average Raman linewidth (FWHH) obtained from four spectra in two bands of polystyrene centered at 1001.34 cm^{-1}

and 1602.40 cm^{-1} was 3.8 cm^{-1} and 5.2 cm^{-1}, respectively. The system was operated with Thermo Fisher OMNIC 8.1 software. Calibration and alignment of the spectrograph were checked using pure polystyrene.

The laser beam was focused at different barbs and barbules until obtaining five single spectra of pheomelanin and/or five single spectra of eumelanin for each feather. The Raman signal was assigned to either pheomelanin or eumelanin on the basis of the diagnostic bands 1 (at 500 cm^{-1} for both pheomelanin and eumelanin), 2 (at 1500 cm^{-1} for pheomelanin and at 1380 cm^{-1} for eumelanin) and 3 (at 2000 cm^{-1} for pheomelanin and at 1580 cm^{-1} for eumelanin)[20] (Fig. 1). These three bands were used to fit Lorentzian deconvolution functions to the Raman curves to obtain spectral parameters derived from each spectrum. From the deconvolution functions, we obtained the following vibrational characteristics for each diagnostic band: spectral position, intensity, width at half maximum and area. For each feather, we calculated the mean of the vibrational characteristics of pheomelanin and eumelanin.

These analyses were made with Thermo Fisher OMNIC 8.1 software. The Peak Resolve routine in OMNIC was used to fit individual synthetic peaks to the complex set of overlapping peaks considering the selected region of the spectra. This algorithm finds peaks on the basis of minima in the Savitzky–Golay second derivative of the selected spectral regions. A polynomial order = 6 was used as a sensitivity parameter for calculating this derivative. The convergence routine in OMNIC is a Fletcher–Powell–McCormick algorithm. Convergence is determined by the ratio of the root mean square (rms) of the residual to the rms of noise in the spectra.

Pigmentation phenotype expression

We used an Ocean Optics (Dunedin, FL, USA) Jaz spectrophotometer (range 220–1000 nm) with UV (deuterium) and visible (tungsten-halogen) lamps and a bifurcated 400 μm fiber optic probe to determine the color expression of the same feathers in which melanin vibrational characteristics were analyzed. The fiber optic probe both provided illumination and obtained light reflected from the sample, with a reading area of *ca.* 1 mm^2. Feathers were mounted on a light absorbing foil sheet (Metal Velvet coating, Edmund Optics, Barrington, NJ, USA) to avoid any background reflectance. Measurements were taken at a 90° angle to the sample. All measurements were relative to a diffuse reflectance standard tablet (WS-1, Ocean Optics), and reference measurements were frequently made. An average spectrum of five readings was obtained for each feather, removing the probe after each measurement. Reflectance curves were obtained by calculating the median of the percent reflectance in 10 nm intervals.

Brightness (*i.e.* summed reflectance across the 300–700 nm spectral range) is the best descriptor of the intensity of melanin-based color expression between feathers of a given species, with lower brightness values indicating higher expression.[51] When feathers significantly differ in hue (*i.e.* perceived color), variation in hue is explained by the slope of the regression of percent reflectance against wavelength.[23] Therefore, as the feathers of the four poultry breeds used in the study show different colors (Fig. 2), we determined the intensity of pigmentation phenotype expression by means of feather brightness controlling for variation in color slope in the statistical analyses (see below).

Systemic oxidative stress

Total glutathione levels (*i.e.* GSH + GSSG) in erythrocytes were determined by following Tietze[52] and Griffith[53] with some particular modifications for bird samples.[54] To determine GSSG levels, 400 μl of the supernatant obtained for the assessment of total glutathione was adjusted to a pH of 7.5 by adding 6 N NaOH. Afterwards, 8 μl of 2-vinylpyridine was added to the aliquot, and the mixture was vigorously shaken at ambient temperature in the dark to promote GSH derivatization. The mixture was then centrifuged at 3500*g* for 10 min, and the change in the absorbance of the supernatant was assessed at 405 nm. GSH levels were calculated by subtracting GSSG levels from total glutathione levels. The ratio GSH : GSSG was used as an index of systemic oxidative stress, with higher ratios indicating lower oxidative stress levels.

Systemic oxidative damage

Cellular oxidative damage was quantified by means of MDA levels in plasma. MDA is an end product of the peroxidation of cellular lipids that occurs as a consequence of attack by ROS and is thus an indicator of ROS-mediated damage at a systemic level.[55] MDA levels in plasma were analyzed by measuring the absorbance at 532 nm of the product generated in the reaction of MDA with thiobarbituric acid, using the lipid peroxidation assay kit of Sigma-Aldrich. Values are expressed as picomoles of MDA per μl of plasma.

Antioxidant capacity

The enzymes SOD and catalase were measured in plasma to account for the capacity of birds to avoid oxidative stress and damage caused by the superoxide radical produced in the mitochondria. SOD activity in plasma was quantified spectrophotometrically by means of the inhibition of reduction of cytochrome *c* by superoxide radicals produced in the xanthine oxidase (XO)-catalysed oxidation of xanthine.[56] Catalase activity in plasma was also determined spectrophotometrically by means of the degree of reduction of potassium permanganate ($KMnO_4$) by H_2O_2 not decomposed by catalase.[57]

Statistical analyses

Vibrational characteristics (spectral position, intensity, width at half maximum and area for each diagnostic Raman band) were highly intercorrelated. Therefore, we analyzed the capacity of these variables to predict variation in mitochondrial ROS (G.M. of DHR or Mitosox fluorescence intensity; response variables) by means of PLSR models. This is an appropriate statistical technique to analyze the predictive capacity of highly intercorrelated predictor variables,[21] and particularly of vibrational characteristics.[20] The extracted PLSR components account for successively lower proportions of original variance, and the relative contribution of each predictor variable to the derived

components is provided by the square of the predictor weights.[21] We controlled for the effects of breed, sex and physical condition by adding these variables as additional predictors to the PLSR models. Different models were fit for pheomelanin and eumelanin vibrational characteristics. Similar models were used to analyze the predicting capacity of oxidative stress (GSH:GSSG) and oxidative damage (MDA levels) by mitochondrial ROS. In these, the G.M. of DHR and Mitosox fluorescence intensity were predictors in the same models, as well as breed, sex and physical condition and the activity level of SOD and catalase and GSH levels (in the model for MDA levels) to account for the antioxidant capacity. PLSR models were also applied to analyze the capacity of vibrational characteristics to predict pigmentation phenotype expression, considering in the models either the light brown color patch or the black color patch of the feathers of the Red Villafranquina breed (Fig. 2). All continuous variables were $\log_{10}$-transformed prior to analyses to achieve normality assumptions. The statistical significance of predictors in the PLSR models (*i.e.* the degree of correlation between the response variable and the predictors) was determined by testing the significance of their regression coefficients by bootstrapping using 100 replications.

Acknowledgements

IG is supported by a Ramón y Cajal Fellowship (RYC-2012-10237) from the Spanish Ministry of Economy and Competitiveness, and funded by the project IN[15]CMA_CMA_1422 from Fundación BBVA ('Convocatoria 2015 de ayudas Fundación BBVA a investigadores y creadores culturales'). The authors thank two anonymous reviewers for constructive comments that improved the manuscript, Javier Cerezo for useful discussions, Francisco Solano for comments on melanocyte extraction, and Rafael Márquez and Sara Borrego for help with laboratory analyses.

References

1 B. C. Stipe, M. A. Rezaei and W. Ho, Single-molecule vibrational spectroscopy and microscopy, *Science*, 1998, **280**, 1732–1735.
2 *Computational Strategies for Spectroscopy: from Small Molecules to Nano Systems*, ed. V. Barone, John Wiley & Sons, Inc., Hoboken, NJ, 2011.
3 J. C. J. Bart and C. H. MacGillavry, The crystal and molecular structure of canthaxanthin, *Acta Crystallogr., Sect. B: Struct. Crystallogr. Cryst. Chem.*, 1968, **24**, 1587–1606.
4 P. Cysewski, Influence of thermal vibrations on aromaticity of benzene, *Phys. Chem. Chem. Phys.*, 2011, **13**, 12998–13008.
5 D. Venkateshvaran, M. Nikolka, A. Sadhanala, V. Lemaur, M. Zelazny, M. Kepa, M. Hurhangee, A. J. Kronemeijer, V. Pecunia and I. Nasrallah, *et al.*, Approaching disorder-free transport in high-mobility conjugated polymers, *Nature*, 2014, **515**, 384–388.
6 W. Bors, W. Heller, C. Michel and M. Saran, Flavonoids as antioxidants: determination of radical-scavenging efficiencies, *Methods Enzymol.*, 1990, **186**, 343–355.
7 K. E. Heim, A. R. Tagliaferro and D. J. Bobilya, Flavonoid antioxidants: chemistry, metabolism and structure–activity relationships, *J. Nutr. Biochem.*, 2002, **13**, 572–584.
8 T. Daniele, I. Hurbain, R. Vago, G. Casari, G. Raposo, C. Tacchetti and M. V. Schiaffino, Mitochondria and melanosomes establish physical contacts modulated by Mfn2 and involved in organelle biogenesis, *Curr. Biol.*, 2014, **24**, 393–403.
9 B. C. Dickinson and C. J. Chang, Chemistry and biology of reactive oxygen species in signaling or stress responses, *Nat. Chem. Biol.*, 2011, **7**, 504–511.
10 M. R. Chedekel, S. K. Smith, P. W. Post, A. Pokora and D. L. Vessell, Photodestruction of pheomelanin: role of oxygen, *Proc. Natl. Acad. Sci. U. S. A.*, 1978, **75**, 5395–5399.
11 S. Takeuchi, W. Zhang, K. Wakamatsu, S. Ito, V. J. Hearing, K. H. Kraemer and D. E. Brash, Melanin acts as a potent UVB photosensitizer to cause a novel mode of cell death in murine skin, *Proc. Natl. Acad. Sci. U. S. A.*, 2004, **101**, 15076–15081.
12 T. Ye, L. Hong, J. Garquilo, A. Pawlak, G. S. Edwards, R. J. Nemanich, T. Sarna and J. D. Simon, Photoionization thresholds of melanins obtained from free electron laser-photoelectron emission microscopy, femtosecond transient absorption spectroscopy and electron paramagnetic resonance measurements of oxygen photoconsumption, *Photochem. Photobiol.*, 2006, **82**, 733–737.
13 I. Galván, A. Bonisoli-Alquati, S. Jenkinson, G. Ghanem, K. Wakamatsu, T. A. Mousseau and A. P. Møller, Chronic exposure to low-dose radiation at Chernobyl favours adaptation to oxidative stress in birds, *Funct. Ecol.*, 2014, **28**, 1387–1403.
14 D. Mitra, X. Luo, A. Morgan, J. Wang, M. P. Hoang, J. Lo, C. R. Guerrero, J. K. Lennerz, M. C. Mihm and J. A. Wargo, *et al.*, An ultraviolet-radiation-independent pathway to melanoma carcinogenesis in the red hair/fair skin background, *Nature*, 2012, **491**, 449–453.
15 A. M. Morgan, J. Lo and D. E. Fisher, How does pheomelanin synthesis contribute to melanomagenesis?, *BioEssays*, 2013, **35**, 672–676.
16 A. Napolitano, L. Panzella, G. Monfrecola and M. d'Ischia, Pheomelanin-induced oxidative stress: bright and dark chemistry bridging red hair phenotype and melanoma, *Pigm. Cell Melanoma Res.*, 2014, **27**, 721–733.
17 L. Panzella, L. Leone, G. Greco, G. Vitiello, G. D'errico, A. Napolitano and M. d'Ischia, Red human hair pheomelanin is a potent pro-oxidant mediating UV-independent contributory mechanisms of melanomagenesis, *Pigm. Cell Melanoma Res.*, 2014, **27**, 244–252.
18 H. Wang, S. Osseiran, V. Igras, A. J. Nichols, E. M. Roider, J. Pruessner, H. Tsao, D. E. Fisher and C. L. Evans, *In vivo* coherent Raman imaging of the melanomagenesis-associated pigment pheomelanin, *Sci. Rep.*, 2016, **6**, 37986.
19 S. M. Robert, S. C. Buckingham, S. L. Campbell, S. Robel, K. T. Holt, T. Ogunrinu-Babarinde, P. P. Warren, D. M. White and M. A. Reid, *et al.*, SLC7A11 expression is associated with

seizures and predicts poor survival in patients with malignant glioma, *Sci. Transl. Med.*, 2015, **7**, 289ra86.
20 I. Galván, A. Jorge, K. Ito, K. Tabuchi, F. Solano and K. Wakamatsu, Raman spectroscopy as a non-invasive technique for the quantification of melanins in feathers and hairs, *Pigm. Cell Melanoma Res.*, 2013, **26**, 917–923.
21 L. M. Carrascal, I. Galván and O. Gordo, Partial least squares regression as an alternative to current regression methods used in ecology, *Oikos*, 2009, **118**, 681–690.
22 I. Galván, A. Jorge, F. Solano and K. Wakamatsu, Vibrational characterization of pheomelanin and trichochrome F by Raman spectroscopy, *Spectrochim. Acta, Part A*, 2013, **110**, 55–59.
23 I. Galván and K. Wakamatsu, Color measurement of the animal integument predicts the content of specific melanin forms, *RSC Adv.*, 2016, **6**, 79135–79142.
24 Y. J. Ai, G. Tian, R. Z. Liao, Q. Zhang, W. H. Fang and Y. Luo, Intrinsic property of flavin mononucleotide controls its optical spectra in three redox states, *ChemPhysChem*, 2011, **12**, 2899–2902.
25 J. Cerezo, J. Zúñiga, A. Requena, F. J. Ávila Ferrer and F. Santoro, Harmonic models in cartesian and internal coordinates to simulate the absorption spectra of carotenoids at finite temperatures, *J. Chem. Theory Comput.*, 2013, **9**, 4947–4958.
26 D. Jacquemin, E. Brémond, I. Ciofini and C. Adamo, Impact of vibronic couplings on perceived colors: two anthraquinones as a working example, *J. Phys. Chem. Lett.*, 2012, **3**, 468–471.
27 P. Mukhopadhyay, M. Rajesh, G. Haskó, B. J. Hawkins, M. Madesh and P. Pacher, Simultaneous detection of apoptosis and mitochondrial superoxide production in live cells by flow cytometry and confocal microscopy, *Nat. Protoc.*, 2007, **2**, 2295–2301.
28 N. W. Kooy, J. A. Royall, H. Ischiropoulos and J. S. Beckman, Peroxynitrite-mediated oxidation of dihydrorhodamine 123, *Free Radical Biol. Med.*, 1994, **16**, 149–156.
29 S. Guglietta, A. Chiavelli, E. Zagato, C. Krieg, S. Gandini, P. S. Ravenda, B. Bazolli, B. Lu, G. Penna and M. Rescigno, Coagulation induced by C3aR-dependent NETosis drives protumorigenic neutrophils during small intestinal tumorigenesis, *Nat. Commun.*, 2016, **7**, 11037.
30 P. Fisicaro, V. Barili, B. Montanini, G. Acerbi, M. Ferracin, F. Guerrieri, D. Salerno, C. Boni, M. Massari and M. C. Cavallo, *et al.*, Targeting mitochondrial dysfunction can restore antiviral activity of exhausted HBV-specific CD8 T cells in chronic hepatitis B, *Nat. Med.*, 2017, **23**, 327–336.
31 H. Swalwell, J. Latimer, R. M. Haywood and M. A. Birch-Machin, Investigating the role of melanin in UVA/UVB-and hydrogen peroxide-induced cellular and mitochondrial ROS production and mitochondrial DNA damage in human melanoma cells, *Free Radical Biol. Med.*, 2012, **52**, 626–634.
32 L. Panzella, G. Gentile, G. D'Errico, N. F. Della Vecchia, M. E. Errico, A. Napolitano, C. Carfagna and M. d'Ischia, Atypical structural and π-electron features of a melanin polymer that lead to superior free-radical-scavenging properties, *Angew. Chem., Int. Ed.*, 2013, **52**, 12684–12687.
33 E. Piskounova, M. Agathocleous, M. M. Murphy, Z. Hu, S. E. Huddlestun, Z. Zhao, A. M. Leitch, T. M. Johnson, R. J. DeBerardinis and S. J. Morrison, Oxidative stress inhibits distant metastasis by human melanoma cells, *Nature*, 2015, **527**, 186–191.
34 A. C. Flor and S. J. Kron, Lipid-derived reactive aldehydes link oxidative stress to cell senescence, *Cell Death Dis.*, 2016, **7**, e2366.
35 C. S. Sander, F. Hamm, P. Elsner and J. J. Thiele, Oxidative stress in malignant melanoma and non-melanoma skin cancer, *Br. J. Dermatol.*, 2003, **148**, 913–922.
36 E. A. Veal, A. M. Day and B. A. Morgan, Hydrogen peroxide sensing and signaling, *Mol. Cell*, 2007, **26**, 1–14.
37 M. d'Ischia, K. Wakamatsu, F. Cicoira, E. Di Mauro, J. C. Garcia-Borron, S. Commo, I. Galván, G. Ghanem, K. Kenzo and P. Meredith, *et al.*, Melanins and melanogenesis: from pigment cells to human health and technological applications, *Pigm. Cell Melanoma Res.*, 2015, **28**, 520–544.
38 E. Cesareo, L. Korkina, G. D'Errico, G. Vitiello, M. S. Aguzzi, F. Passarelli, J. Z. Pedersen and A. Facchiano, An endogenous electron spin resonance (ESR) signal discriminates nevi from melanomas in human specimens: a step forward in its diagnostic application, *PLoS One*, 2012, **7**, e48849.
39 M. I. Franco, L. Turin, A. Mershin and E. M. Skoulakis, Molecular vibration-sensing component in *Drosophila melanogaster* olfaction, *Proc. Natl. Acad. Sci. U. S. A.*, 2011, **108**, 3797–3802.
40 F. F. Crim, Chemical dynamics of vibrationally excited molecules: Controlling reactions in gases and on surfaces, *Proc. Natl. Acad. Sci. U. S. A.*, 2008, **105**, 12654–12661.
41 W. Zhang, H. Kawamata and K. Liu, CH stretching excitation in the early barrier F+ CHD3 reaction inhibits CH bond cleavage, *Science*, 2009, **325**, 303–306.
42 A. D. Dunkelberger, B. T. Spann, K. P. Fears, B. S. Simpkins and J. C. Owrutsky, Modified relaxation dynamics and coherent energy exchange in coupled vibration-cavity polaritons, *Nat. Commun.*, 2016, **7**, 13504.
43 A. Shalabney, J. George, J. Hutchison, G. Pupillo, C. Genet and T. W. Ebbesen, Coherent coupling of molecular resonators with a microcavity mode, *Nat. Commun.*, 2015, **6**, 5981.
44 S. Ito, K. Wakamatsu, M. d'Ischia, A. Napolitano and A. Pezzella, Structure of melanins, in *Melanins and Melanosomes: Biosynthesis, Biogenesis, Physiological, and Pathological Functions*, ed. J. Borovanský and P. A. Riley, Wiley-Blackwell, Weinheim, 2011, pp. 167–185.
45 S. G. Dávila, M. García-Gil, P. Resino-Talaván and J. L. Campo, Association between polymorphism in the melanocortin 1 receptor gene and E locus plumage color phenotype, *Poult. Sci.*, 2014, **93**, 1089–1096.
46 S. J. Lin, J. Foley, T. X. Jiang, C. Y. Yeh, P. Wu, A. Foley, C. M. Yen, Y. C. Huang, H. C. Cheng and C. F. Chen, *et al.*, Topology of feather melanocyte progenitor niche allows complex pigment patterns to emerge, *Science*, 2013, **340**, 1442–1445.
47 S. Mohanty, A. Kumar, J. Dhawan, V. Sreenivas and S. Gupta, Noncultured extracted hair follicle outer root sheath cell

suspension for transplantation in vitiligo, *Br. J. Dermatol.*, 2011, **164**, 1241–1246.
48 C. Lerner, A. Bitto, D. Pulliam, T. Nacarelli, M. Konigsberg, H. V. Remmen, C. Torres and C. Sell, Reduced mammalian target of rapamycin activity facilitates mitochondrial retrograde signaling and increases life span in normal human fibroblasts, *Aging Cell*, 2013, **12**, 966–977.
49 M. Xu, X. X. Li, J. Xiong, M. Xia, E. Gulbins, Y. Zhang and P. L. Li, Regulation of autophagic flux by dynein-mediated autophagosomes trafficking in mouse coronary arterial myocytes, *Biochim. Biophys. Acta, Mol. Cell Res.*, 2013, **1833**, 3228–3236.
50 I. Galván and A. Jorge, Dispersive Raman spectroscopy allows the identification and quantification of melanin types, *Ecol. Evol.*, 2015, **5**, 1425–1431.
51 K. J. McGraw, R. J. Safran and K. Wakamatsu, How feather colour reflects its melanin content, *Funct. Ecol.*, 2005, **19**, 816–821.
52 F. Tietze, Enzymatic method for quantitative determination of nanogram amounts of total and oxidized glutathione: applications to mammalian blood and other tissues, *Anal. Biochem.*, 1969, **27**, 502–522.
53 O. W. Griffith, Determination of glutathione and glutathione disulfide using glutathione reductase and 2-vinylpyridine, *Anal. Biochem.*, 1980, **106**, 297–312.
54 I. Galván and C. Alonso-Alvarez, The expression of melanin-based plumage is separately modulated by exogenous oxidative stress and a melanocortin, *Proc. R. Soc. B*, 2009, **276**, 3089–3097.
55 D. Weismann, K. Hartvigsen, N. Lauer, K. L. Bennett, H. P. Scholl, P. C. Issa, M. Cano, H. Brandstätter, S. Tsimikas and C. Skerka, *et al.*, Complement factor H binds malondialdehyde epitopes and protects from oxidative stress, *Nature*, 2011, **478**, 76–81.
56 J. M. McCord and I. Fridovich, Superoxide dismutase. An enzymic function for erythrocuprein (hemocuprein), *J. Biol. Chem.*, 1969, **244**, 6049–6055.
57 G. Cohen, D. Dembiec and J. Marcus, Measurement of catalase activity in tissue extracts, *Anal. Biochem.*, 1970, **34**, 30–38.